

# Triply differential photoelectron studies of non-Franck-Condon behavior in the photoionization of acetylene

A. C. Parr and D. L. Ederer

*Synchrotron Ultraviolet Radiation Facility, National Bureau of Standards, Washington, D.C. 20234*

J. B. West

*Daresbury Laboratory, Daresbury, Warrington, WA4 4AD England*

D. M. P. Holland

*Institute of Physical Science and Technology, University of Maryland, College Park, Maryland 20742*

J. L. Dehmer

*Argonne National Laboratory, Argonne, Illinois 60439*

(Received 30 November 1981; accepted 29 December 1981)

Vibrational branching ratios and photoelectron angular distributions for alternative vibrational levels of  $C_2H_2^+$   $X^2\Pi_u$  have been measured in the range  $13\text{ eV} \leq h\nu \leq 25\text{ eV}$  using synchrotron radiation. Below  $h\nu \sim 16\text{ eV}$ , these data exhibit strong non-Franck-Condon effects, namely, wavelength-dependent vibrational branching ratios, and vibrational-state-dependent photoelectron asymmetry parameters. Moreover, enhanced excitation of bending modes of the ion is observed below  $h\nu \sim 16\text{ eV}$ , in addition to the C-C stretch mode, which is the only mode readily observed in photoelectron spectra of  $C_2H_2$  at shorter wavelengths, e.g., at the He I (21.2 eV) resonance line. The non-Franck-Condon behavior is attributed to resonant photoionization processes, whose identification is discussed in the framework of several recent theoretical and experimental studies on acetylene and related molecules.

## I. INTRODUCTION

Recent experimental<sup>1-15</sup> and theoretical<sup>16-25</sup> work has underscored the importance of using vibrational branching ratios and photoelectron angular distributions as probes of shape and autoionizing resonances in molecular photoionization. Both resonant processes induce large departures of the vibrational branching ratios from those based on Franck-Condon (FC) factors and produce photoelectron asymmetry parameters which depend strongly on the vibrational state of the ion. These non-FC effects probe the resonant processes in a more detailed, hence more sensitive way than do vibrationally unresolved studies of partial cross sections and angular distributions.

In the case of shape resonances, recent theoretical predictions<sup>16,17</sup> of non-FC effects were quickly verified experimentally<sup>3-6</sup> in diatomic cases. As for non-FC effects caused by autoionization, definitive theoretical work has only been completed on  $H_2$  photoionization,<sup>20,23</sup> which, owing to the need for improved wavelength resolution at high flux, has heretofore eluded a direct test by means of triply differential photoelectron experiments. Experiments on  $N_2$ ,<sup>8,11</sup>  $O_2$ ,<sup>10</sup> etc., have however, produced clear experimental evidence of the type of non-FC behavior to expect near autoionization features. Moreover, cases have been identified<sup>7,15,21,24,25</sup> in which it is likely that the non-FC effects entail intermingling of shape and autoionizing resonances in the same spectral range. This more complex, hybrid resonant behavior has yet to be treated theoretically.

With this background in smaller molecules, it seems

appropriate to extend the study of resonance-induced non-FC effects in molecular photoionization to larger polyatomics, for which autoionizing states are universal, of course, and shape resonances are present in most molecules. In this paper, we present new data on  $C_2H_2$ , which represents a logical extension to polyatomics as it is isoelectronic with  $N_2$  and CO, which are understood rather well. The present experiments are triply differential photoelectron measurements on the  $X^2\Pi_u$  state of  $C_2H_2^+$  over the range  $13\text{ eV} \leq h\nu \leq 25\text{ eV}$ . That is, photoelectron spectra were recorded as a function of three independent variables—incident wavelength, ejection angle, and kinetic energy—using synchrotron radiation and a rotating electron spectrometer with sufficient resolving power to resolve the major vibrational progression in the  $X^2\Pi_u$  state of  $C_2H_2^+$ . Of particular interest in  $C_2H_2$  is the broad dip (or alternatively, double bump) structure in the photoionization spectrum<sup>26-29</sup> at  $h\nu \sim 14\text{ eV}$ . Recent theoretical<sup>9,12,22,29,30</sup> and experimental<sup>9,12-14,30</sup> work has addressed the question of the nature of the origin of the prominent feature(s)—shape resonant, autoionization, or some combination—but no consensus exists, even at the qualitative level. The only certainty is that a band of resonant structure dominates the spectrum from the I. P. to  $\sim 16\text{ eV}$ . Indeed, we find major non-FC effects in both vibrational branching ratios and  $v$ -dependent  $\beta$ 's for the major C-C stretching mode in this wavelength range. Moreover, we report previously unobserved enhancement of bending modes in this same region. These modes are very weak at shorter wavelengths, and, in fact, have only recently been observed<sup>31</sup> in the

584 Å photoelectron spectrum. Although we are unable to satisfactorily resolve these modes in the present experiment, our analysis clearly demonstrates that they become comparable in intensity to members of the dominant C–C stretch mode below  $h\nu \sim 16$  eV. Clearly, the complete separation and quantitative measurement of these modes are clear priorities for future high-resolution work. In the meantime, the data presented here will help resolve the nature of the structure near  $h\nu \sim 14$  eV by serving as a detailed check of theoretical work on the dominant C–C stretch mode. In addition to presenting these new data, we discuss the various possible mechanisms for the observed non-FC effects, in light of recent ideas and theoretical work. Although certain key elements of the resonant mechanisms have been satisfactorily established, e.g., the important contribution of the  $2\sigma_u^{-1}1\pi_g$  autoionizing state, other conflicting conclusions remain to be resolved by future theoretical work, preferably at the multichannel level so as to take full advantage of the detailed dynamical information implicit in the triply differential data presented here and elsewhere.<sup>14</sup>

## II. EXPERIMENTAL

The apparatus used in this work has been described in detail elsewhere<sup>32</sup> and will only be discussed briefly here. The variable wavelength light was obtained from a high-aperture 2 m, normal-incidence monochromator<sup>33</sup> attached to the National Bureau of Standards (SURF-II) storage ring. With a 1200 line/mm grating, a virtual entrance slit (the stored electron orbit) and a 100  $\mu$  exit slit, this instrument produced a spectral resolution of 0.4 Å FWHM and a flux of  $3 \times 10^{10}$  photons  $s^{-1} \text{Å}^{-1}$  at 600 Å with a typical 10 mA beam circulating in the storage ring. The ejected electrons were energy analyzed by a 2 in. mean-radius hemispherical analyzer<sup>34</sup> operated at a constant resolution of  $\sim 110$  meV. The analyzer was calibrated using Ar gas, whose photoionization cross section<sup>35</sup> and photoelectron asymmetry parameters<sup>36,37</sup> are known in this wavelength range. As the light from the monochromator was elliptically polarized, the differential cross section in the dipole approximation, assuming randomly oriented target molecules, can be written<sup>32,38</sup>

$$\frac{d\sigma}{d\Omega} = (\sigma_{\text{tot}}/4\pi)[1 + \frac{1}{4}\beta(3P \cos 2\theta + 1)], \quad (1)$$

where  $\beta$  is the photoelectron asymmetry parameter,  $\theta$  is the photoelectron ejection angle relative to the major polarization axis, and  $P = (I_{\parallel} - I_{\perp})/(I_{\parallel} + I_{\perp})$  is the polarization of the light which was measured with a three-mirror polarization analyzer.<sup>32</sup> At each wavelength reported here, photoelectron spectra encompassing the  $X^2\Pi_u$  band of  $C_2H_2^+$  were recorded at  $\theta = 0^\circ$ ,  $45^\circ$ , and  $90^\circ$ . At each angle, the spectra were decomposed into vibrational components by means of a nonlinear least-squares fit to Gaussian line shapes after correcting for the transmission function of the electron spectrometer and a small  $< 4\%$  angular correction factor based on the electron spectrometer calibration. The asymmetry parameter  $\beta$  was then determined for each vibrational component by means of Eq. (1), and vibrational branching ratios were determined by comparing the component

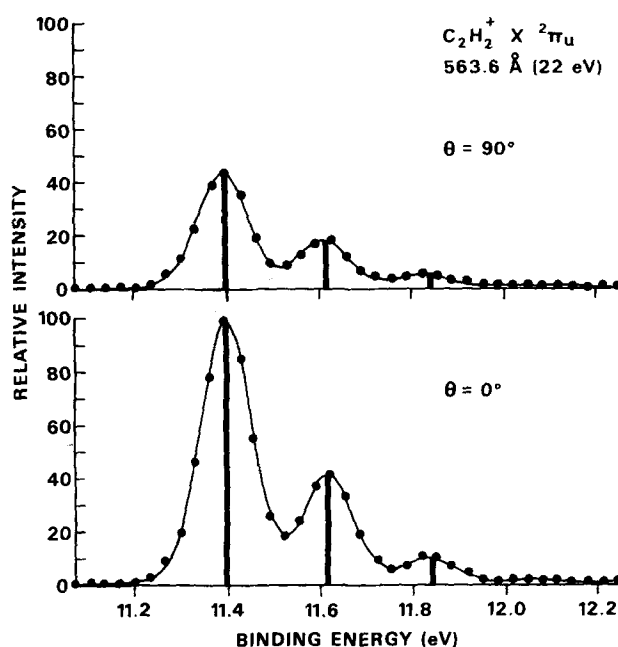


FIG. 1. Photoelectron spectra of  $C_2H_2^+ X^2\Pi_u$  at  $h\nu = 22.0$  eV and at  $\theta = 0^\circ$  and  $90^\circ$ . Both spectra are normalized so that the maximum counts in the  $\theta = 0^\circ$  spectra equals 100. The data points (●) and nonlinear least-squares fit curve (—) are indicated. The amplitudes and positions of the C–C stretch vibrational components yielded by the fit are represented by the vertical solid bars.

intensities at the magic angle  $\theta = 54.7^\circ$ , as deduced from Eq. (1), using the intensities at the measured angles and the measured  $\beta$  values. The errors quoted in the next section represent a combination of the uncertainty of the nonlinear least-squares fit and the degree of agreement between the parameters deduced from the redundant set of measurements at three angles.

## III. RESULTS

The crux of the analysis of the present data is the appreciation that the importance of alternative vibrational modes of the ion can vary drastically in different parts of the spectrum. In particular, predication of the analysis on the fact that the previously published He I photoelectron spectrum<sup>39</sup> of the  $X^2\Pi_u$  band of  $C_2H_2^+$  exhibits clearly only excitation of the C–C stretching mode would lead to erroneous analysis of the spectra for  $h\nu < 16$  eV where resonant excitation has been found here to lead to substantial excitation of other modes, i.e., bending modes. In fact, this observation, documented below for  $C_2H_2^+$  is probably the rule rather than the exception for variable-wavelength studies of polyatomics, for which allowance must always be made for enhanced excitation of vibrational modes, which have very small Franck–Condon factors and hence are often difficult to detect in photoelectron spectra at nonresonant wavelengths.

To illustrate this, we show angle-resolved photoelectron spectra of  $C_2H_2^+ X^2\Pi_u$  at  $\lambda = 563.6$  Å (22.0 eV) and at  $\lambda = 885.6$  Å (14.0 eV) in Figs. 1 and 2, respectively. At  $h\nu = 22$  eV (Fig. 1), a single 0.222 eV vibrational spacing, corresponding to the C–C stretch mode, ade-

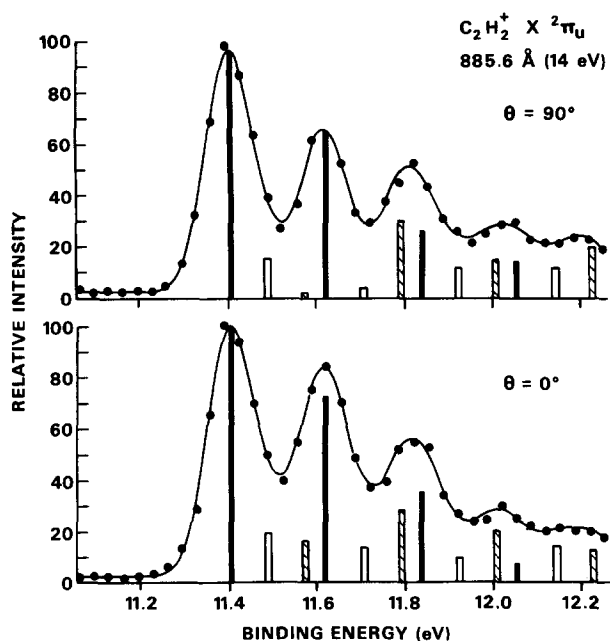


FIG. 2. Photoelectron spectra of  $C_2H_2^+ X^2\Pi_u$  at  $h\nu = 14$  eV and at  $\theta = 0^\circ$  and  $90^\circ$ . Both spectra are normalized so that the maximum counts in the  $\theta = 0^\circ$  spectra equals 100. The data points (●) and nonlinear least-squares fit curve (—) are indicated. The amplitudes and positions of the vibrational components yielded by the fit are as follows: solid bars, C—C stretch; clear bars, 0.086 eV bending mode; crosshatched bar, 0.172 eV harmonic of bending mode.

quately describes the observed spectrum. Use of this single mode, together with a constant peak width of  $\sim 120$  meV and a background level determined at the extremities of the data in Fig. 1, results in an excellent least-squares fit and is in agreement with the He I photoelectron spectrum.<sup>39</sup> (In Fig. 1, the solid line is the spectrum generated by the least-squares fit and the vertical solid bars indicate the position and relative strengths of the members of the C—C stretch progression.) Below  $h\nu = 16$  eV, however, this analysis procedure was found to be inadequate: The peak positions of the higher members of the progression appeared shifted, the valleys between the peaks appeared to fill in more than the resolution or background level warranted, and the quality-of-fit parameter degraded significantly. The key to this puzzle was supplied by a recent high-resolution, high-sensitivity He I photoelectron spectrum<sup>31</sup> which indicated the location of previously unobserved bending modes of the ground state of  $C_2H_2^+$  with intensities at the  $\sim 1\%$  level. The observed vibrational spacings were 0.036, 0.086, and 0.172 eV, which might plausibly correspond to a *trans*-bending mode and a *cis*-bending mode and its harmonic. The first of these is too close to the main C—C stretch progression to be separated with the resolution of the present experiment; however, when the 0.086 and 0.172 eV modes were added to the fitting procedure, the fit quickly converged with a quality-of-fit parameter equal to the high-energy ( $h\nu > 16$  eV) fits. The result is illustrated in Fig. 2 for  $h\nu = 14.0$  eV, where the 0.222, 0.086, and 0.172 eV vibrational progressions are indicated by solid, clear,

and hatched bars, respectively. Again, the vertical bars indicate the spectral position and relative intensities of the various vibrational components, and the solid line is the spectral shape of the band generated by the least-squares fit. In comparing Figs. 1 and 2, note particularly the reduced peak-to-valley ratio and the shift of the experimental peaks away from the C—C stretch components in Fig. 2. The cause for the changes in the spectral shape and peak positions is clearly attributable to the enhanced excitation of the bending modes in the low-energy portion of the excitation spectrum. In fact, transitions involving resonant excitation of bending vibrations become comparable to or even dominate higher members of the main progression at certain wavelengths. Another qualitative observation made clear by Figs. 1 and 2 is that the lower-energy spectrum is more isotropic than the higher-energy spectrum, i.e., has a lower  $\beta$  value.

In Figs. 3 and 4, we present the spectral variation of the vibrational branching ratios and  $v$ -dependent  $\beta$ 's for the dominant C—C stretch mode of  $C_2H_2^+ X^2\Pi_u$  in the range  $13 \text{ eV} \leq h\nu \leq 25 \text{ eV}$ . Although Fig. 2 demonstrates the importance of the bending modes for  $h\nu < 16$  eV, the branching ratios and  $\beta$ 's deduced from the least-squares fit were not of sufficient quality to clearly establish the spectral variation of these parameters in the  $h\nu < 16$  eV region, where they were excited with appreciable intensity. That is, they were usually of less statistical quality than the  $v_2 = 2$  C—C stretch data in Figs. 3 and 4. Also, they are excited almost exclusively by resonant excitation and tend to vary more sharply than the FC-allowed C—C stretch mode. Hence, they should be mapped on a finer energy mesh. Therefore, we confine further discussion of resonance effects to the stronger C—C stretch mode, whose analysis has nevertheless been improved by including the bending frequencies in the fit for  $h\nu < 16$  eV. We stress, therefore, that future higher-resolution work remains to be done for  $h\nu < 16$  eV to completely characterize the photoionization dynamics of this transition in  $C_2H_2$ .

Focusing on the spectral behavior of the C—C stretch mode (referred to simply as  $v_2 = 0, 1, 2$  from now on) in Figs. 3 and 4, we can make the following general observations. First, in Fig. 3, the vibrational branching ratios exhibit different profiles in the  $h\nu < 16$  eV region and converge to constant values for  $h\nu > 16$  eV. Thus, they exhibit non-Franck-Condon behavior below  $h\nu = 16$  eV, and FC behavior above. For example, the  $v_2 = 0$  curve exhibits a local dip at  $h\nu \sim 13.8$  eV, whereas the  $v_2 = 1$  and 2 curves show an enhancement; and the  $v_2 = 0$  is enhanced near  $h\nu = 15$  eV, at which energy the  $v_2 = 1$  curve dips and the  $v_2 = 2$  curve stays flat. Second, the spectral variation of the non-FC branching ratios in Fig. 3 are generally similar to the spectral variation of the "peak" intensities reported by Unwin *et al.*,<sup>9,12</sup> however, the present branching ratios are believed to be representative of a simple C—C stretching mode (with some admixture of the weak 0.036 eV bending mode), since we have separated it from the other vibrational modes which we have determined to be non-negligible in this spectral range. The  $v_2 = 1$  and 2 data of Unwin *et al.*<sup>9,12</sup> could be expected to be affected by this consid-

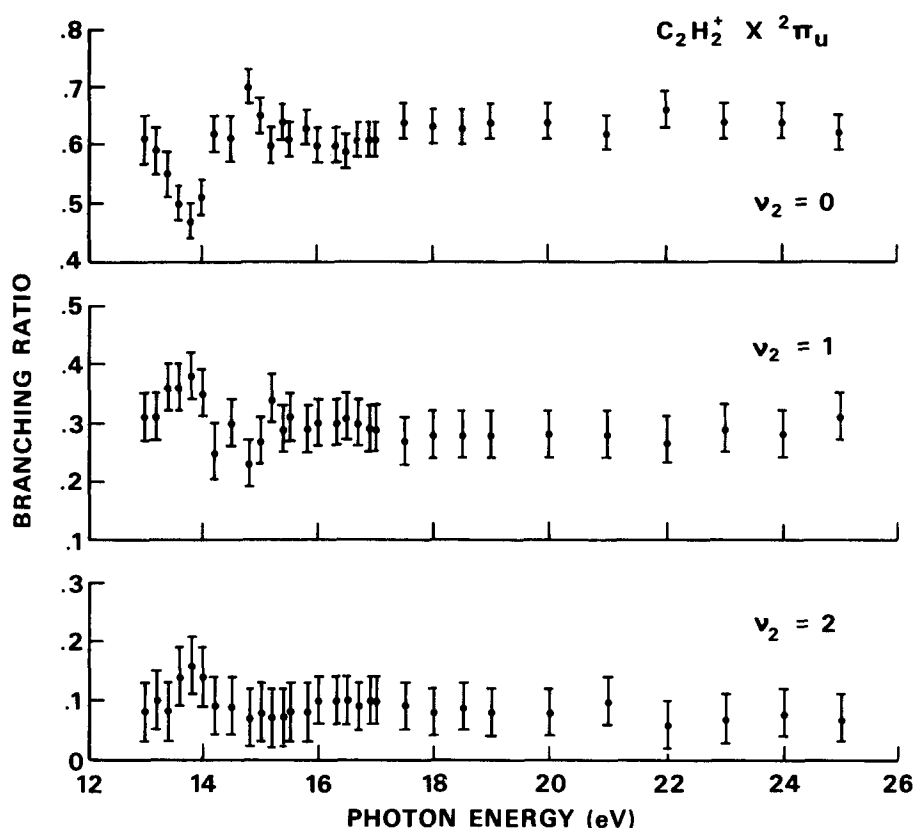


FIG. 3. Vibrational branching ratios for the  $v_2=0$ , 1, and 2 symmetric stretch components of  $C_2H_2^+ X^2\Pi_u$ .

eration. Above  $h\nu \sim 16$  eV, where the excitation of bending modes and other manifestations of resonant excitation are no longer apparent, our branching ratios agree well with those measured by Kreile, Schweig, and Thiel<sup>30</sup> at the Ne I (16.67 and 16.85 eV), He I (21.22 eV), and Ne II (26.81 and 26.91 eV) resonance lines, and with branching ratios derived from FC factors<sup>26,40</sup> ( $v_2=0$ , 0.69,  $v_2=1$ , 0.21,  $v_2=2$ , 0.09). Third, in Fig. 4, the  $v_2=0$  and 1  $\beta$  curves show a distinct broad dip to below  $\beta=0$ , centered at  $h\nu \sim 14.25$  eV and  $h\nu \sim 14.5$  eV, respectively, while the  $v_2=2$  curve fluctuates near  $\beta=0$ , although the statistical uncertainty prohibits a clear picture of the variation of  $v_2=2$  for  $h\nu < 16$  eV. Keep in mind that peaks with small FC factors like  $v_2 \geq 2$  and the bending modes will tend to be populated mainly by resonant processes and, hence, may show much sharper variation within Rydberg series than do the FC-allowed channels. Fourth, all three  $\beta$  curves in Fig. 4 rise at higher energy with grossly similar spectral shape, within error limits, to a value near  $\beta \sim 1$ . Note that photoionization of the  $1\pi_u$  level of  $N_2$  and the  $1\pi$  level of CO, both isoelectronic with  $C_2H_2$ , also result in a vibrationally summed  $\beta$ , which exhibits a general rise from  $\beta=0$  to  $\beta \sim 1$  over the same kinetic energy range.<sup>41,42</sup> This rough correlation among similar orbitals in the three isoelectronic molecules for the non-resonant part of the spectrum seems reasonable. Fifth, comparison of our  $\beta$  values with the resonance line work of Kreile, Schweig, and Thiel<sup>30</sup> confirms the overall accuracy of the independent measurements: The agreement is excellent at all overlapping wavelengths, even at Ar II (13.30 and 13.48 eV), for which comparison is hazardous owing to differences in photon bandpass and

the failure to take bending vibrations into account in Ref. 30. Furthermore, measurements at the Ne II (26.8 and 26.9 eV) and He II (40.8 eV) resonance lines give (roughly  $v_2$  independent)  $\beta$  values of  $\sim 1.4$  and  $\sim 1.6$ , respectively, indicating that the trend observed above is continued to higher energy.

#### IV. DISCUSSION

The main issue to be resolved enroute to the eventual full multichannel analysis of the present data is the nature of the resonant excitation mechanism(s) which induce the non-FC behavior reported here. For instance, to what extent do autoionizing or shape resonances, or a hybrid of both, contribute to the non-FC effects, and what are their symmetries and spectral locations? Such a mechanistic picture is essential in order to carry out a realistic model calculation of even the gross structure in the triply differential results presented in Figs. 3 and 4. Unfortunately, although several theoretical studies have dealt with aspects of this problem at the single channel level, no unified interpretation emerges. Rather, two overlapping, yet substantively differing pictures can be identified. Moreover, the present data cannot yet be used to resolve the outstanding differences since the theoretical work has not incorporated channel interaction into a vibrationally and angularly resolved treatment. Hence, for now, we can only summarize briefly the two points-of-view, in turn, for later testing.

One plausible interpretation of the  $13 \text{ eV} \leq h\nu \leq 16 \text{ eV}$  region of the  $C_2H_2$  photoionization spectrum can be derived from the following composite of recent experimental and theoretical evidence: *First*, recent studies

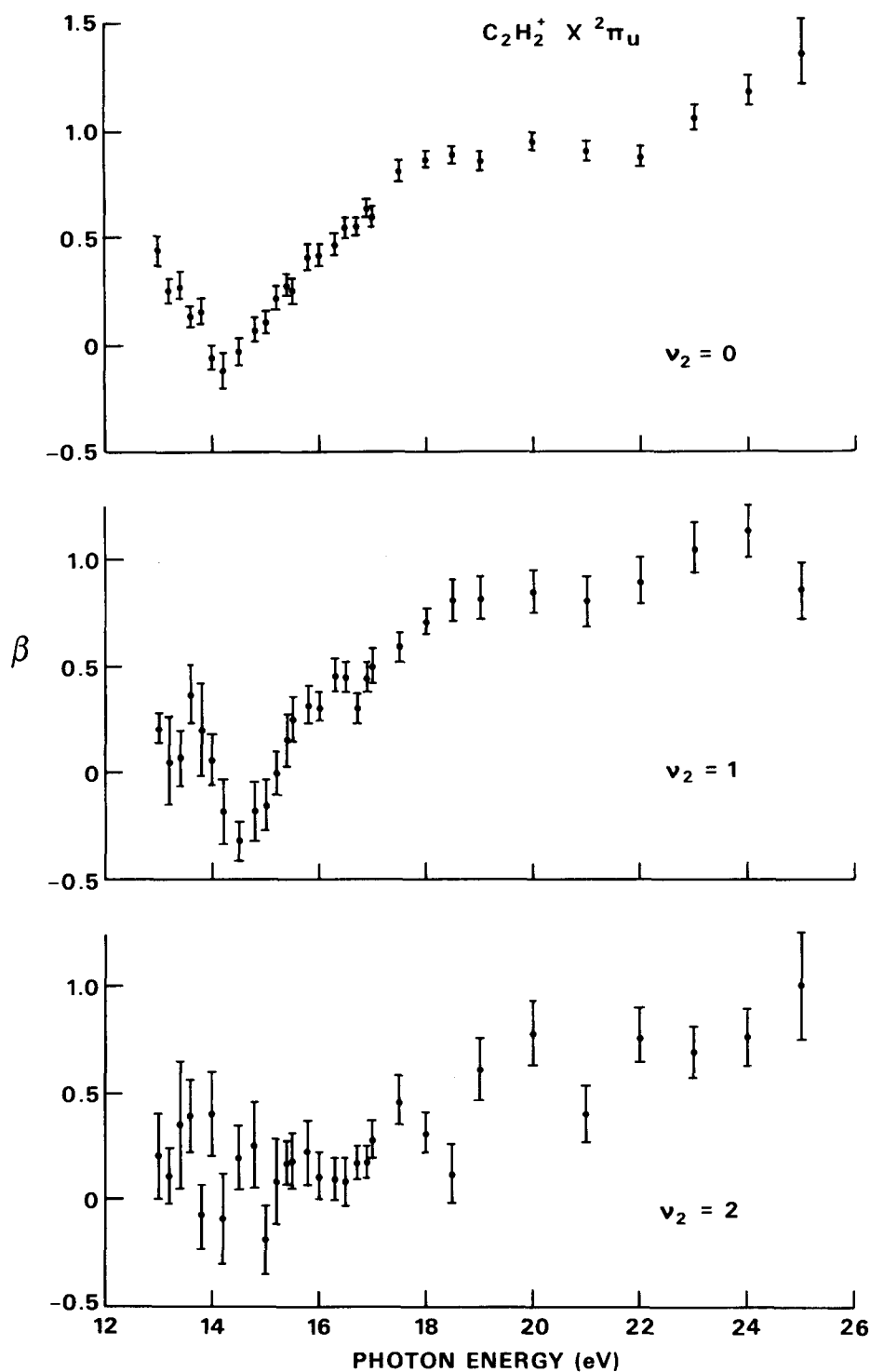


FIG. 4. Photoelectron asymmetry parameters  $\beta$  for the  $\nu_2=0, 1$ , and 2 symmetric stretch components of  $C_2H_2^+ X^2\Pi_u$ .

of the photoionization spectrum of  $C_2H_2$ , by photoionization mass spectrometric methods,<sup>26-29</sup> reveal two broad intense peaks at 930 Å (13.33 eV) and 810 Å (15.31 eV) with some superimposed weak, sharp Rydberg structure starting at 870 Å (14.25 eV) and continuing to shorter wavelength. The nature of the two strong bands is the major object of this discussion. *Second*, recent theoretical photoionization calculations<sup>22</sup> at the Hartree-Fock level account for only a nonresonant background in this region of the photoionization spectrum of  $C_2H_2$ , indicating that the two intense peaks are not accounted for

in a single-channel description of the  $1\pi_u$  photoionization channel, and in particular, that they do not seem to arise from shape resonances in the dipole-allowed  $1\pi_u \rightarrow \epsilon\sigma_g$ ,  $\epsilon\pi_g$ , or  $\epsilon\delta_g$  one-electron continua. This is not surprising in view of the following point. *Third*, shape resonance-enhanced features in the isoelectronic molecules  $N_2$  and  $CO$  occur in the  $\pi_g$  and  $\sigma_u$  final-state symmetries (see, e.g., Refs. 16-18, 43-50). This is most clearly seen in the  $K$ -shell spectra,<sup>43-45,47</sup> in which an extremely intense  $\pi_g(\pi^*)$  peak lies *below* its respective ionization threshold and a  $\sigma_u$  shape resonance lies  $\sim 10$

eV above the I. P. Each is resonantly enhanced by a centrifugal barrier acting on the  $l=2$  component of the  $\pi_g$  state and the  $l=3$  component of the  $\sigma_u$  continuum. In applying this information to  $C_2H_2$ , allowance must be made for the dependence of shape resonances on the molecular field, including changes of nuclear types and geometry. *Fourth*, very recent *ab initio* molecular orbital calculations<sup>29</sup> have shown that two intense transitions converging to the  $3\sigma_g^{-1}2\Sigma_g$  (16.36 eV) and the  $2\sigma_u^{-1}2\Sigma_u$  (18.38 eV) states of  $C_2H_2^+$  are expected to lie at the approximate locations of the two observed strong peaks. These transitions are of the type  $3\sigma_g \rightarrow 3\sigma_u(\sigma^*)$  and  $2\sigma_u \rightarrow 1\pi_g(\pi^*)$  and are expected to be broad owing to strong geometry changes in the excited states. This recent study also made plausible assignments of the Rydberg structure in this region.

Based on these results, the following picture emerges: The strong broad feature at 810 Å (15.31 eV) corresponds<sup>29</sup> to the transition  $2\sigma_u \rightarrow 1\pi_g(\pi^*)$  to an autoionizing valence state converging to the  $2\sigma_u^{-1}2\Sigma_u$  state of the ion. Its large oscillator strength (theoretical value<sup>29</sup> = 0.429) and the absence of significant Rydberg structure in the same channel, indicates that the final state is (shape) resonantly enhanced by a centrifugal barrier associated with the  $l=2$  component. This is consistent with the behavior of the isoelectronic molecules  $N_2$  and CO, as stated above, and is also verified by the carbon  $K$ -shell spectrum<sup>51</sup> of  $C_2H_2$ . The 930 Å (13.33 eV) feature is likewise broad and somewhat less intense (theoretical oscillator strength<sup>29</sup> = 0.1623). It has been assigned<sup>29</sup> to the transition  $3\sigma_g \rightarrow 3\sigma_u(\sigma^*)$  associated with the second electronic state of the ion  $C_2H_2^+ 3\sigma_g^{-1}2\Sigma_g$ . It is doubtful that this transition's strength is caused by shape resonant type enhancement since, in the isoelectronic molecules  $N_2$  and CO, the  $l=3$  shape-resonant activity occurs ~10 eV above the respective I. P. This mechanism of enhancement cannot be ruled out without direct theoretical evidence, however, since changes in nuclear types and separations and in electron correlation within the  $3\sigma_g^{-1}3\sigma_u$  configuration could alter the location of the resonant activities relative to that in  $N_2$  and CO. The carbon  $K$ -shell spectrum<sup>51</sup> is not definitive in this case, since prominent features below and just above threshold and a very weak broad feature ~15 eV above threshold have yet to be definitively assigned. Much of the sharp Rydberg structure in this region has been accounted for by means of  $np\pi_u$  and  $np\sigma_u$  Rydberg states<sup>29</sup> converging to the  $3\sigma_g^{-1}2\Sigma_g$  state of the ion. As we do not resolve this structure in the present work, we will not discuss this fine structure further.

Against this background, we can now compare and contrast recent results by Langhoff *et al.*<sup>12</sup> based on "vertical electronic, separated-channel, static exchange approximation" calculations employing  $L^2$  computational methodology in conjunction with the Stieltjes-Tchebycheff moment theory: *First*, this calculation also identifies a  $2\sigma_u \rightarrow 1\pi_g(\pi^*)$  transition at  $h\nu = 15.54$  eV, with a very large oscillator strength,  $f = 0.8036$ . Thus, both recent theoretical calculations place an extremely intense  $2\sigma_u \rightarrow 1\pi_g(\pi^*)$  transition very near the 810 Å (15.3 eV) feature in the total photoionization spectrum. When this is combined with supporting evidence from spectra

of  $N_2$  and CO, cited above, we can conclude that this (shape) resonantly enhanced autoionizing state is a well-established element of the interpretation of this region of the  $C_2H_2$  photoionization spectrum. *Second*, this calculation places the  $3\sigma_g \rightarrow 3\sigma_u(\sigma^*)$  transition just above the  $3\sigma_g$  ionization threshold rather than near  $h\nu \sim 13.9$  eV as in Ref. 29. This would result in little contribution from this transition to the non-FC effects below  $h\nu \sim 16$  eV. Some support for this is provided by the  $3\sigma_g$  partial cross section<sup>12</sup> which exhibits a broad peak near threshold. On the other hand, Langhoff *et al.*<sup>12</sup> report a  $3\sigma_g \rightarrow 3p\sigma_u$  transition to a Rydberg state at  $h\nu = 13.66$  eV, with an  $f$  number of 0.1480. This is close to the  $3\sigma_g \rightarrow 3\sigma_u(\sigma^*)$  transition reported in Ref. 29 in both  $f$  number and spectral location. This may be merely a terminology problem resulting from differences in the theoretical approaches used. In any case, both works indicate a fairly strong transition in the vicinity of the 930 Å peak in the total photoionization spectrum, which can be expected to have a major impact in that region of the spectrum, although its potential contribution is not explicitly pointed out in Ref. 12. *Third*, the  $1\pi_u \rightarrow \epsilon\sigma_g$ ,  $\epsilon\pi_g$ , and  $\epsilon\delta_g$  continua are found in Ref. 12 to account for the average strength of the  $1\pi_u$  partial cross section, with the double hump structure manifesting itself as a modulation about this average due to channel interaction. This suggests very strong, destructive interference between intense autoionizing features and the underlying continuum, whereas the interpretation described earlier suggests two strong autoionizing features interacting more weakly with a smaller nonresonant background. This is a significant point of disagreement, both in terms of interaction strength and oscillator strength. *Fourth*, Langhoff *et al.*<sup>12</sup> suggest a possible contribution of a  $2\sigma_u \rightarrow 4\sigma_g(\sigma^*)$  transition at  $h\nu \sim 17.68$  eV with an  $f$  number of 0.1551 to the non-FC effects; however, the main non-FC behavior is confined to lower excitation energies, so that the data do not confirm this suggestion in any simple direct way.

Hence, the sum of recent experimental and theoretical evidence results in an unsettled picture in which certain key elements have been clarified, but other important discrepancies remain. The main interpretive progress is that two strong autoionizing transitions  $2\sigma_u \rightarrow 1\pi_g(\pi^*)$  and  $3\sigma_g \rightarrow 3\sigma_u(\sigma^*)$  or  $3p\sigma_u$  are major contributors to the non-FC effects in the  $13 \text{ eV} \leq h\nu \leq 16 \text{ eV}$  region of the  $C_2H_2$  spectrum, and that the  $1\pi_g(\pi^*)$  is resonantly enhanced by the action of a centrifugal barrier on its  $l=2$  component. Otherwise, shape resonance effects appear to be absent.

Obviously, further experimental and theoretical work is needed to produce a complete analysis of the photoionization dynamics of  $C_2H_2$  in this spectral range. For example, a critical test of the tentative ideas discussed above would involve realistic calculations of the triply differential results presented in Figs. 3 and 4. Such spectrally, vibrationally, and angularly resolved photoelectron spectra constitute a very detailed probe of the photoionization dynamics, and necessitate a more precise modeling of the process than do total photoionization cross sections. On the experimental side, two important improvements must be made to further clarify

our understanding. First, measurements on a finer wavelength mesh and with improved resolution would help separate the effects of Rydberg structure from the gross behavior of the two main features. In Figs. 3 and 4, some localized fluctuations may, in fact, result from hitting autoionizing features. Second, measurements with higher electron kinetic energy resolution are needed to document the branching ratios and angular distributions for the enhanced excitations of bending modes for  $h\nu \leq 16$  eV, which we were able to detect but not map out. Such comments are sure to apply to other studies of polyatomic molecules, whose detailed study, at the level reported here has just begun. The ongoing, rapid progress in similar studies at synchrotron light sources will no doubt make rapid strides in this direction.

## ACKNOWLEDGMENTS

We wish to thank R. P. Madden for his support and encouragement and the staff of the NBS SURF-II facility for their valuable assistance. This work was supported in part by the Office of Naval Research, the U. S. Department of Energy, and NATO Grant No. 1939.

- <sup>1</sup>P. R. Woodruff and G. V. Marr, Proc. R. Soc. London Ser. A **358**, 87 (1977).
- <sup>2</sup>J. L. Gardner and J. A. R. Samson, J. Electron Spectrosc. **13**, 7 (1978).
- <sup>3</sup>R. Stockbauer, B. E. Cole, D. L. Ederer, J. B. West, A. C. Parr, and J. L. Dehmer, Phys. Rev. Lett. **43**, 757 (1979).
- <sup>4</sup>J. B. West, A. C. Parr, B. E. Cole, D. L. Ederer, R. Stockbauer, and J. L. Dehmer, J. Phys. B **13**, L105 (1980).
- <sup>5</sup>B. E. Cole, D. L. Ederer, R. Stockbauer, K. Codling, A. C. Parr, J. B. West, E. D. Poliakoff, and J. L. Dehmer, J. Chem. Phys. **72**, 6308 (1980).
- <sup>6</sup>T. A. Carlson, M. O. Krause, D. Mehaffy, J. W. Taylor, F. A. Grimm, and J. D. Allen, J. Chem. Phys. **73**, 6056 (1980).
- <sup>7</sup>P. Morin, I. Nenner, P. M. Guyon, O. Dutuit, and K. Ito, J. Chim. Phys. **77**, 605 (1980).
- <sup>8</sup>A. C. Parr, D. L. Ederer, B. E. Cole, J. B. West, R. Stockbauer, K. Codling, and J. L. Dehmer, Phys. Rev. Lett. **46**, 22 (1981).
- <sup>9</sup>R. Unwin, I. Khan, N. V. Richardson, A. M. Bradshaw, L. S. Cederbaum, and W. Domcke, Chem. Phys. Lett. **77**, 242 (1981).
- <sup>10</sup>K. Codling, A. C. Parr, D. L. Ederer, R. Stockbauer, J. B. West, B. E. Cole, and J. L. Dehmer, J. Phys. B **14**, 657 (1981).
- <sup>11</sup>J. B. West, K. Codling, A. C. Parr, D. L. Ederer, B. E. Cole, R. Stockbauer, and J. L. Dehmer, J. Phys. B **14**, 1791 (1981).
- <sup>12</sup>P. W. Langhoff, B. V. McKoy, R. Unwin, and A. M. Bradshaw, Chem. Phys. Lett. **83**, 270 (1981).
- <sup>13</sup>A. C. Parr, D. L. Ederer, R. Stockbauer, J. B. West, K. Codling, D. M. P. Holland, and J. L. Dehmer, *XII International Conference on the Physics of Electronic and Atomic Collisions, Book of Abstracts*, July 15–21, 1981; Gatlinburg, Tennessee, p. 81.
- <sup>14</sup>T. A. Carlson, F. A. Grimm, D. Mehaffy, P. R. Keller, J. W. Taylor, M. O. Krause, and J. D. Allen, Jr., *XII International Conference on the Physics of Electronic and Atomic Collisions, Book of Abstracts*, July 15–21, 1981, Gatlinburg, Tennessee, p. 83; J. Electron Spectrosc. (in press).
- <sup>15</sup>P. Morin, I. Nenner, P. M. Guyon, L. F. A. Ferreira, and K. Ito, *XII International Conference on the Physics of Electronic and Atomic Collisions, Book of Abstracts*, July 15–21 1981, Gatlinburg, Tennessee, p. 87.
- <sup>16</sup>J. L. Dehmer, D. Dill, and S. Wallace, Phys. Rev. Lett. **43**, 1005 (1979).
- <sup>17</sup>J. L. Dehmer and D. Dill, in *Electronic and Atomic Collisions*, edited by N. Oda and K. Takayanagi (North-Holland, Amsterdam, 1980), p. 195.
- <sup>18</sup>G. Raseev, H. LeRouzo, and H. Lefebvre-Brion, J. Chem. Phys. **72**, 5701 (1980).
- <sup>19</sup>J. R. Swanson, D. Dill, and J. L. Dehmer, J. Phys. B **14**, L207 (1981).
- <sup>20</sup>M. Raoult and Ch. Jungen, J. Chem. Phys. **74**, 3388 (1981).
- <sup>21</sup>G. Raseev, H. Lefebvre-Brion, H. LeRouzo, and A. L. Roche, J. Chem. Phys. **74**, 6686 (1981).
- <sup>22</sup>R. R. Lucchese and V. McKoy, *XII International Conference on the Physics of Electronic and Atomic Collisions, Book of Abstracts*, July 15–21 1981, Gatlinburg, Tennessee, p. 80.
- <sup>23</sup>M. Raoult, Ch. Jungen, and D. Dill, J. Chim Phys. Paris **77**, 599 (1980).
- <sup>24</sup>J. A. Stephens, D. Dill, and J. L. Dehmer, J. Phys. B **14**, 3911 (1981).
- <sup>25</sup>P. M. Dittman, D. Dill, and J. L. Dehmer, J. Chem. Phys. (in press).
- <sup>26</sup>R. Botter, V. H. Dibeler, J. A. Walker, and H. M. Rosenstock, J. Chem. Phys. **44**, 1271 (1966).
- <sup>27</sup>J. E. Collin and J. Delwiche, Can. J. Chem. **45**, 1883 (1967).
- <sup>28</sup>J. Berkowitz, *Photoabsorption, Photoionization, and Photoelectron Spectroscopy* (Academic, New York, 1979), pp. 284–290.
- <sup>29</sup>T. Hayaishi, S. Iwata, M. Sasanuma, E. Ishiguro, Y. Morioko, Y. Iida, and M. Nakamura, J. Phys. B (in press).
- <sup>30</sup>J. Kreile, A. Schweig, and W. Thiel, Chem. Phys. Lett. **79**, 547 (1981).
- <sup>31</sup>P. M. Dehmer and J. L. Dehmer, J. Electron Spectrosc. (to be published).
- <sup>32</sup>A. C. Parr, R. L. Stockbauer, B. E. Cole, D. L. Ederer, J. L. Dehmer, and J. B. West, Nucl. Instrum. Methods **172**, 357 (1980).
- <sup>33</sup>D. L. Ederer, B. E. Cole, and J. B. West, Nucl. Instrum. Methods **172**, 185 (1980).
- <sup>34</sup>J. L. Dehmer and D. Dill, Phys. Rev. A **18**, 164 (1978).
- <sup>35</sup>G. V. Marr and J. B. West, At. Data Nucl. Data Tables **18**, 497 (1976).
- <sup>36</sup>J. Kreile and A. Schweig, J. Electron Spectrosc. **20**, 191 (1980).
- <sup>37</sup>D. M. P. Holland, A. C. Parr, D. L. Ederer, J. L. Dehmer, and J. B. West, Nucl. Instrum. Methods (in press).
- <sup>38</sup>J. A. R. Samson and A. F. Starace, J. Phys. B **8**, 1806 (1975).
- <sup>39</sup>C. Baker and D. W. Turner, Proc. R. Soc. London Ser. A **308**, 19 (1968).
- <sup>40</sup>V. H. Dibeler and J. A. Walker, Int. J. Mass. Spectrom. Ion Phys. **11**, 49 (1973).
- <sup>41</sup>S. Wallace, D. Dill, and J. L. Dehmer, J. Phys. B **12**, L417 (1979).
- <sup>42</sup>R. M. Holmes and G. V. Marr, J. Phys. B **13**, 945 (1980).
- <sup>43</sup>G. R. Wight, C. E. Brion, and M. J. van der Wiel, J. Electron Spectrosc. **1**, 457 (1973).
- <sup>44</sup>J. L. Dehmer and D. Dill, Phys. Rev. Lett. **35**, 213 (1975).
- <sup>45</sup>J. L. Dehmer and D. Dill, J. Chem. Phys. **65**, 5327 (1976).
- <sup>46</sup>J. A. R. Samson, G. N. Haddad, and J. L. Gardner, J. Phys. B **10**, 1749 (1977).
- <sup>47</sup>R. B. Kay, Ph. E. van der Leeuw, and M. J. van der Wiel, J. Phys. B **10**, 2513 (1977).
- <sup>48</sup>E. W. Plummer, T. Gustafsson, W. Gudat, and D. E. Eastman, Phys. Rev. A **15**, 2339 (1977).
- <sup>49</sup>T. N. Rescigno, C. F. Bender, B. V. McKoy, and P. W. Langhoff, J. Chem. Phys. **68**, 970 (1978).
- <sup>50</sup>N. Padiyal, G. Csanak, B. V. McKoy, and P. W. Langhoff, J. Chem. Phys. **69**, 2992 (1978).
- <sup>51</sup>A. P. Hitchcock and C. E. Brion, J. Electron Spectrosc. **10**, 317 (1977).